Single-Cycle Plain-Woven Objects

Qing Xing[1], Ergun Akleman[2], Jianer Chen[3], Jonathan L. Gross[4]
[1]Architecture Department, Texas A&M University
[2]Visualization Department, Texas A&M University
[3]Computer Science Department, Texas A&M University
[4]Computer Science Department, Columbia University

***Abstract*—It has recently been shown that if we twist an arbitrary subset of edges of a mesh on an orientable surface, the resulting extended graph rotation system (EGRS) can be used to induce a cyclic weaving on the surface. In extended graph rotation systems, an edge is viewed as a paper strip that can be twisted. The sides of the paper strips provide "two strands" to construct weaving structures. Either these strands are "parallel" to the mesh edge for an "untwisted edge", or they both cross over the edge and over each other for a "twisted edge". If an arbitrary subset of edges of a mesh on an orientable surface is twisted in the same helical sense, then the EGRS induces a cyclic plain-weaving on the surface, which consists of cycles that cross other cycles (or themselves) by alternatingly going over and under.**

In this paper, we show that it is always possible to create a single-cycle plain-weaving starting from a mesh on an arbitrary surface, by selecting an appropriate subset of edges to be twisted. We also demonstrate how, starting from a mesh, to construct a large number of single-cycle plain-woven objects. Interestingly, the single-cycle solutions with a minimal number of edge twists correspond to plain-woven objects that are visually similar to Celtic knots.

For converting plain-weaving cycles to 3D thread structures, we extend the original projection method, which previously worked only when all mesh edges are twisted. With the extension described here, our projection method can also be used to handle untwisted edges. We have developed a system that converts any manifold mesh into single-cycle plain-woven objects, by interactively controlling the proportion of edges that are twisted. The system also allows us to change the shapes of the threads with a set of parameters, interactively in real-time. We demonstrate here that by using this system, we can create a wide variety of single-cycle plain-woven objects.

1. Introduction

A *plain-woven* object consists of threads that are interlaced so that a traversal of each thread alternatingly goes over and under the other threads (or itself) as it crosses them. It has recently been shown how to create plain-woven objects from any given manifold mesh surface, by constructing an alternating projection of a link on the surface. It has also been shown how to create such plain-woven objects from any given manifold mesh by twisting some of the edges of a related orientable manifold mesh [1], [2]. Akleman et al. showed that twisting all the edges of a manifold mesh is a useful approach for creating objects that visually resemble plain-weaving. Nonetheless, there are two problems with twisting all the edges: (1) it does not control the number of cycles that will be created, and (2) the visual results are too uniform. On the other hand, if we randomly twist some of the edges, we can get interesting results, as shown in Figure 2. However, random twisting does not control the number of cycles. In this paper, we develop a method that allows us to control the number of cycles in a plain-weaving, which, in particular, enables us to construct single-cycle plain-weavings on an arbitrary surface. We also show that there exist a large number of single-cycle plain-weaving structures and that some of the single-cycle plain-weaving structures visually resemble Celtic knots (See Figure 1).

Twisting all the edges of a manifold mesh is theoretically related to drawing Celtic knots in 2D using planar graphs [3], [4]. Twisting all edges makes the resulting weaving visually look like physical weaving. However, we have noticed that to visually achieve the look of Celtic knots in 3D, we need to leave many edges untwisted. One problem with leaving many edges untwisted is that the resulting weaving can be a separable link, which means that a sphere can be inserted into 3D-space that does not intersect the link, such that part of the link lies on one side of the separation and part on the other (See Figure 2). A separable link will fall apart if it is physically realized. By reducing the number of components of the link to one, we guarantee that physical structure will not fall apart.

The mathematical links without solid shape need to be converted to 3D thread structures, such as extruded lines (ribbons) or extruded surfaces (yarns). The projection (PR) method introduced in [1] for converting mathematical links to 3D thread structures is provided only for twisted edges. Since we use untwisted edges in this paper, there is a need to extend the projection method to handle untwisted edges.

As a practical implementation, we have developed a system that converts any manifold mesh into a single-cycle plain-woven object. Our system converts the mathematical knots and links to 3D thread structures, such that the shapes of the threads can be interactively

978-0-7695-4072-6/10 $26.00 © 2010 IEEE
DOI 10.1109/SMI.2010.13

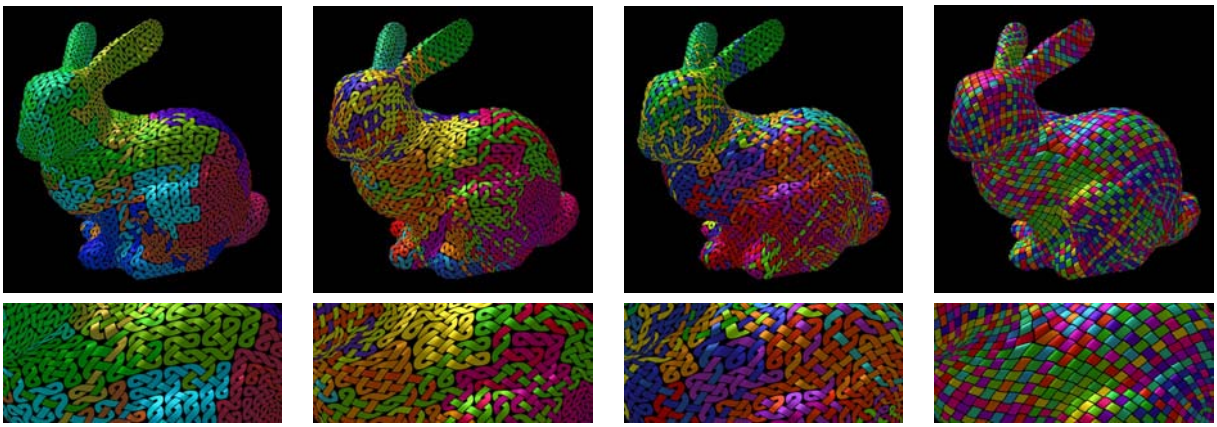

54.99% twisted | 65.61% twisted | 75.02% twisted | 99.83% twisted

Fig. 1. *Rainbow colored single-cycle plain-woven bunnies. Each bottom image magni es the detail of the single-cycle plain-woven bunny immediately above. The number below each bottom image indicates the percentage of edges that are twisted. These details illustrate how the percentage of twisted edges impacts the visual results. We painted the single thread with rainbow colors to better illustrate its structure.*

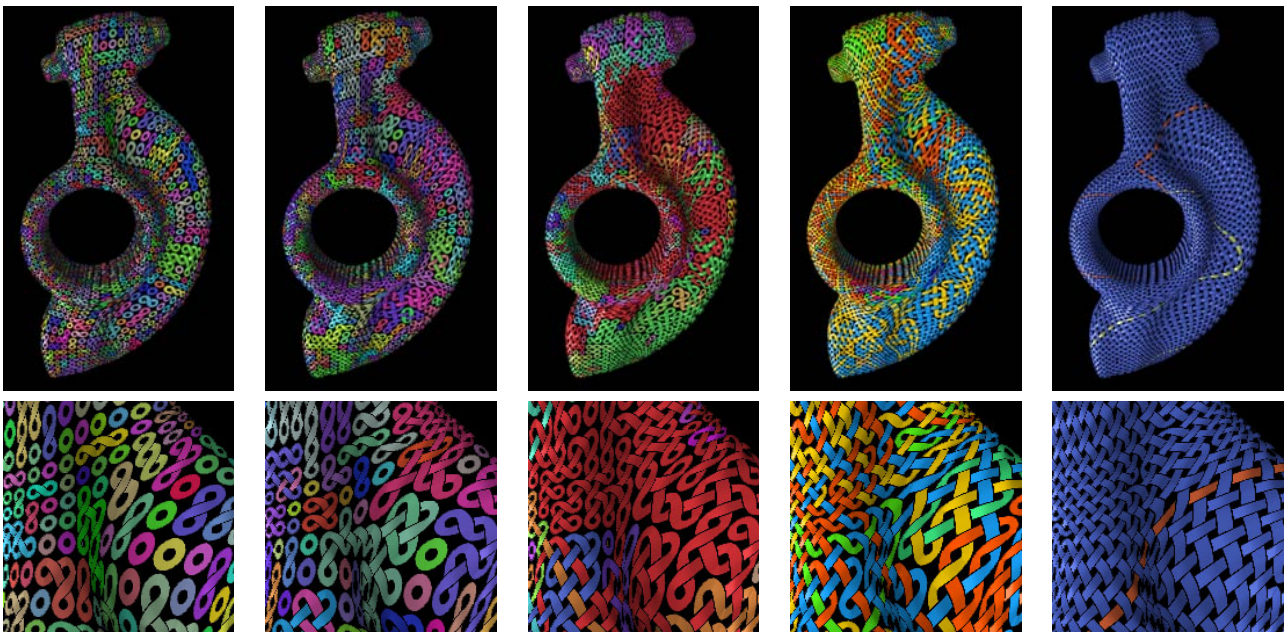

20% twisted, 3138 cycles | 40% twisted, 1351 cycles | 60% twisted, 346 cycles | 80% twisted, 35 cycles | 98% twisted, 3 cycles

Fig. 2. *Random twisting with no cycle control. Each bottom image is magni ed detail from the plain-woven Rockarm object immediately above. The number below a bottom image indicates the percentage of edges that are twisted and the number of cycles. These details illustrate how the percentage of twisted edges impacts the visual results.*

controlled with a set of parameters. The 3D structure of the single thread can cover the original orientable manifold mesh, without leaving large gaps. In Section 3, we provide examples of some single-cycle plain-woven objects. In addition, we show in Section 4 that the number of single-cycle solutions are statistically high. Section 5 gives our conclusions and describes possibilities for future work.

2. Theory for Single-Cycle Weaving

As introduced formally in [1], a *cyclic plain-weaving* on an orientable surface S_o is a projection of a link L on S_o, such that (1) there are no triple intersections at any single point of S_o, and (2) a traversal of the image on S_o of each component of L goes over and under alternatingly as it crosses the images of other components or of itself.

Graph Rotation Systems have been a powerful model in the study of topological graph theory [5], [6], [7], [8]. A *rotation at a vertex* of a graph is a cyclic ordering of

the set of the edge-ends that are incident at that vertex. It is well-known (see Theorem 3.2.2 of [5]) that a rotation system specifies a graph embedding and that every graph embedding can be specified by a rotation system.

Akleman et al. introduced extended graph rotation systems [2] to facilitate a representation of cyclic weaving in which edge twists are used to create crossings in a weaving. In extended graph rotation systems, an edge is viewed as a paper strip that can be twisted clockwise or counter-clockwise in helical sense (see Figure 3). The sides of the paper strips provides "two strands" in the generated weaving pattern. These strands are either "parallel" to the mesh edge for an "untwisted edge", or they both cross over the edge and over each other for a "twisted edge". The type of the crossover depends on helical twist type (i.e. clockwise or counter-clockwise). If an arbitrary subset of edges of a mesh on an orientable surface S_o is twisted in the same helical sense, then the GRS induces a cyclic plain-weaving on S_o [2].

Formally, let $\rho_o(G)$ be a graph rotation system with no twisted edges, which corresponds to an embedding of the graph G on an orientable surface S_o. Let A be an arbitrary subset of edges of G. Twisting all edges in A in the same helical sense (i.e. either clockwise or counter-clockwise; see Figure 3) gives an *extended graph rotation system* $\rho(G)$. The face tracing algorithm [1] applied on $\rho(G)$ returns all face boundaries for the faces in $\rho(G)$, which can be regarded as cycles mapped to the surface S_o (See Figure 4). These cycles mapped on S_o make a cyclic plain-weaving W on the surface S_o. We say that the cyclic plain-weaving W is *induced* by the extended graph rotation system $\rho(G)$.

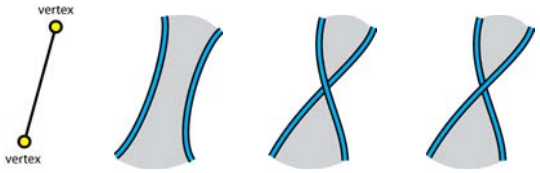

(a) Edge (b) 0 Twisted (c) +1 Twisted (d) -1 Twisted

Fig. 3. *In computer graphics, an edge is usually drawn as shown in (a) and it is not considered to be twisted. In extended graph rotation systems, an edge is viewed as a paper strip that can be twisted clockwise or counter-clockwise. (b) shows a visual interpretation of an untwisted edge, which is called 0-twisted. In plain-weaving, twisted edges can only be in one of two possible states. These states are shown in (c) $+1$ (i.e. counter-clockwise) twisted or (d) -1 (i.e. clockwise) twisted.*

To construct a plain-weaving based on the projection method proposed in [1], Akleman et al. suggested that all edges of the mesh be twisted. In particular, it was left unspecified how the projection method should be applied if certain edges are untwisted. In this paper, we extend the projection method and allow some edges to be left

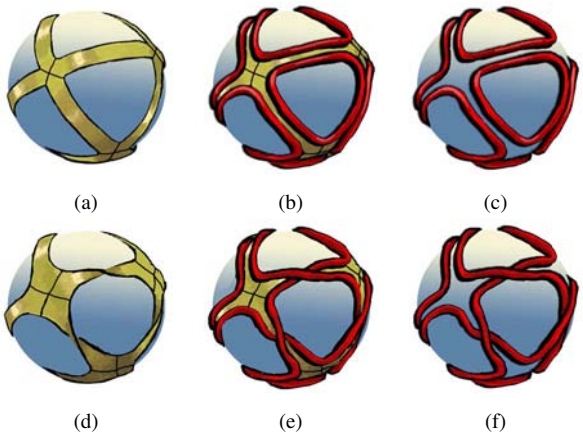

Fig. 4. *An example of creating plain-weaving on a surface with face tracing. The mesh in (a) is an octahedron constructed by untwisted edges embedded in a sphere. As shown in (c), the eight face-boundary walks of the octahedron are unlinked in 3D. However, if some edges are twisted as shown in (d), then the cycles represented by the boundary walks become linked, as in (f).*

untwisted. By controlling which edges are to be twisted, we create single-cycle plain-woven objects. Edmonds proved that every connected graph has a one-face non-orientable embedding [9]. The following theorem that is a weaving version of Edmonds' theorem is fundamental to this paper.

Theorem 2.1: Let $\rho(G)$ be a graph rotation system that is obtained from a mesh on a surface S_o by possibly twisting some of its edges. Suppose that the cyclic plain-weaving induced by $\rho(G)$ has at least two distinct cycles. Let e be an edge in G whose two sides belong to two different cycles c_1 and c_2 in the weaving. If we twist e , then we combine the two cycles c_1 and c_2 into one cycle and reduce the number of cycles in the weaving by one. Using this procedure, we can always reduce the number of cycles in a weaving to one.

Proof: In a graph rotation system, if an edge at the intersection of two faces is twisted, the two faces are merged into one face[1]. Since cycles are simply the boundaries of faces, twisting an edge combines the two cycles that correspond to the boundaries of the two faces. Since the surface S_o is connected, we can always find an edge e whose two sides belong to two cycles of $\rho(G)$. Therefore, we can always reduce the number of cycles to one. ■

The single-cycle plain-weaving structures that are created by this procedure are topological knots and do not have shape in space. In order to create geometric forms, these knots need to be converted into 3D thread structures, such as ribbons (extruded lines) or yarns

[1]If e is already twisted, twist operation untwist the edge e. Similarly, if the original edge e is untwisted, twist operation makes e twisted. Also note that in both GRS and EGRS, a face is considered as the domain that always lies on one (either left-hand or right-hand) side of a thread, as one traverses one of cycles of the weaving.

(extruded polygons). The resulting 3D thread structures must look smooth and must not self-intersect. For conversion of topological links into geometric forms, we need to extend the projection method introduced in [1], so that it will work well for untwisted edges.

3. Extending the Projection Method to Untwisted Edges

For a rotation system $\rho_0(G)$, we consider only the polygonal mesh surfaces, where every vertex has valence at least 3, every face has at least three sides (i.e. triangles), every edge has positive length, and every vertex has position information. Whereas Akleman et al. gave a detailed explanation of the projection method for twisted edges, here we explain how to handle both twisted and untwisted edges. Moreover, in addition to explaining the method in 3D, we provide explanation for a mesh in the plane, which can provide a better understanding of the process.

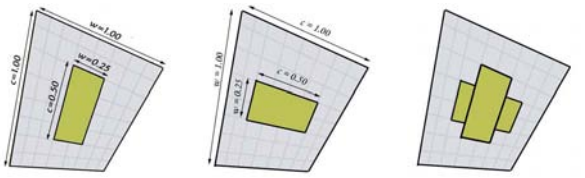

(a) Top (b) Bottom (c) Together

Fig. 6. *Strip construction with c and w control for twisted case.*

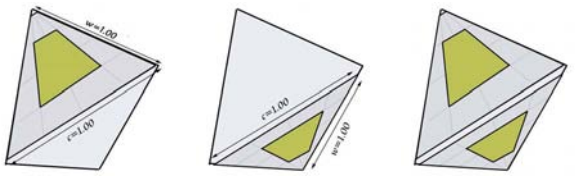

(a) One Side (b) Other side (c) Together

Fig. 7. *Strip construction with c and w control for untwisted case.*

Figure 5 shows the steps of the extended projection method for a mesh in the plane with one untwisted edge. The procedure consists of five steps as follows:

1) Project the initial mesh to a local plane. The result will locally be a planar tiling as shown in Figure 5(a).
2) Connect the center of each face to the vertices of that face, thereby forming a quadrilateral for each edge. Graph theorists call this construction the *radial graph* of the embedding. In Figure 5(b) small black dots identify the centers of the faces (called "face-points" of the radial graph) and the vertex positions (called "vertex-points"). Figure 5(c) and (d) show the 24 quadrilaterals constructed by joining the face-points and the vertex points for every edge. These quadrilaterals are called *edge-regions*.
3) a) For every twisted edge, project the corresponding edge-region to two small planar regions, one slightly above and the other slightly below the original plane shown in Figure 6(a) and (b).
   b) For every untwisted edge, create two side-by-side quadrilaterals in the original plane. These are triangular-looking shapes that are shown in Figure 7(a) and (b). Each quadrilateral consists of the original edge and two vertices that are co-located in the center of its corresponding face. Since two vertices are co-located in the center of the face, the procedure yields a quadrilateral instead of a triangle. Figure 5(e) shows projected edge regions for one untwisted edge and for the other edges twisted.
4) Using the projected edge regions (i.e. quadrilaterals) as control shapes, we form strips by using a simple bilinear equation. Figures 6 and 7 show how the strips are formed for the twisted and untwisted cases.
   a) For twisted edges, the procedure shown in Figure 6(a) and (b) creates two strips that are on top of each other, forming an " " shape as shown in Figure 6(c). We calculate the 4 corners of the yellow quadrilateral regions, in barycentric coordinates inside two grey quadrilaterals slightly above and below the original plane. The positions of these corner points is parameterized by two parameters w and c. The value of w controls the width of the yellow quadrilateral region, and the value of c controls the length of the yellow quadrilateral region. Note that to compute the upper and lower yellow quadrilateral regions, we switch c and w values, which gives us " " shape shown in Figure 6(c).
   b) For untwisted edges, the procedure shown in Figure 7(a) and (b) creates two strips that are side-by-side as shown in Figure 7(c). Figure 5(f) shows all strips: " " shapes for twisted edges and two parallel strips for the untwisted edges. We again calculate the 4 corners of the yellow quadrilateral regions, in barycentric coordinates inside the grey triangle-looking quadrilaterals. The value of w again controls the width of the yellow quadrilateral region, and the value of c controls the length of the yellow quadrilateral region. On the other hand, to compute the two

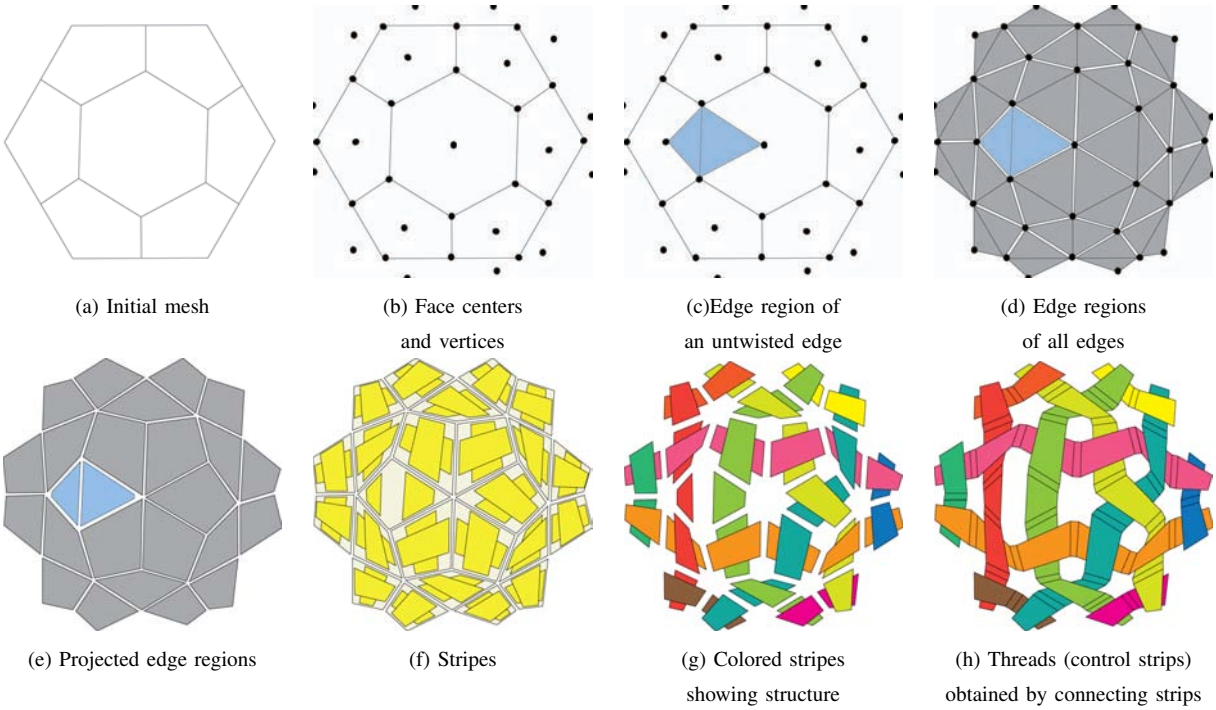

(a) Initial mesh (b) Face centers and vertices (c)Edge region of an untwisted edge (d) Edge regions of all edges

(e) Projected edge regions (f) Stripes (g) Colored stripes showing structure (h) Threads (control strips) obtained by connecting strips

Fig. 5. *The steps of the projection method for a planar mesh with only one untwisted edge.*

side-by-side yellow quadrilateral regions, we use c and w values exactly the same way, which gives us two "parallel strands" shown in Figure 7(c).

5) Connect the strips to form a ring of polygon strip, which we call a "control strip", which is used to control the shape of the threads. These polygons are smoothed to create the final ribbons or yarns. Note that the shape of the control strip is defined by the parameters w and c, where w is the locally adjusted width of the ribbon which is relative to the size of underlying edges, and c controls the steepness of the transition between the upper and the lower offset levels.
6) Smooth the control strip. A variety of approaches, such as B-Spline or Bezier curves, can be employed to create smooth ribbons. To create smooth yarns, first convert the control strip to control yarns and then smooth the control yarns using a subdivision scheme. For details see [1].

3.1 Examples and Results

We have developed a system that converts polygonal meshes to single-cycle plain-woven objects. We provide two parameters c and w to change the steepness c and local width (or thickness) w of ribbons. A user can interactively change the parameters c and w to achieve different results. A dense weaving is obtained with $c \approx 1$ and $w \approx 1$. Small values of c and w provide sparse weaving. All the plain-woven object images in this paper are direct screen captures from the system. They were all created in real-time. In the case of multiple-cycle weaving structures, the colors of the thread cycles are randomly chosen. For single-cycle woven objects, we changed the hue of the ribbon color (rainbow coloring) along the cycle to show the structure. The projection algorithm guarantees that the sizes of strips are relative to the underlying polygons. Therefore, the actual widths of the ribbons vary in different parts of the mesh.

The projection method can close the gaps by creating a dense look, as shown in Figures 8, and 9. Figures 1 and 10 include close-up images that show the visual results impacted by percentage of twisting. Figures 11 and 12 show the single-cycle plain-weaving results coming from meshes that are not quadrilaterals. For pleasing looking results it is desirable to start with a mesh with fairly uniform edge lengths and with no very acute angles in any of the facets. The projection method closes the gaps better if the angle θ between two faces on the two sides of the edge [1], is between 120^0 and 180^0. The closer that θ approaches 180^0, the better it is for closing gaps. This can be achieved with a few applications of a suitable subdivision scheme. For example, using the Doo-Sabin scheme, after each subdivision all θ values become closer to 180^0, while the faces become more nearly regular, more nearly convex, and more nearly planar. We do not provide direct self-intersection avoidance; however, choosing values of c and w between 0 and 1 is sufficient to avoid self-

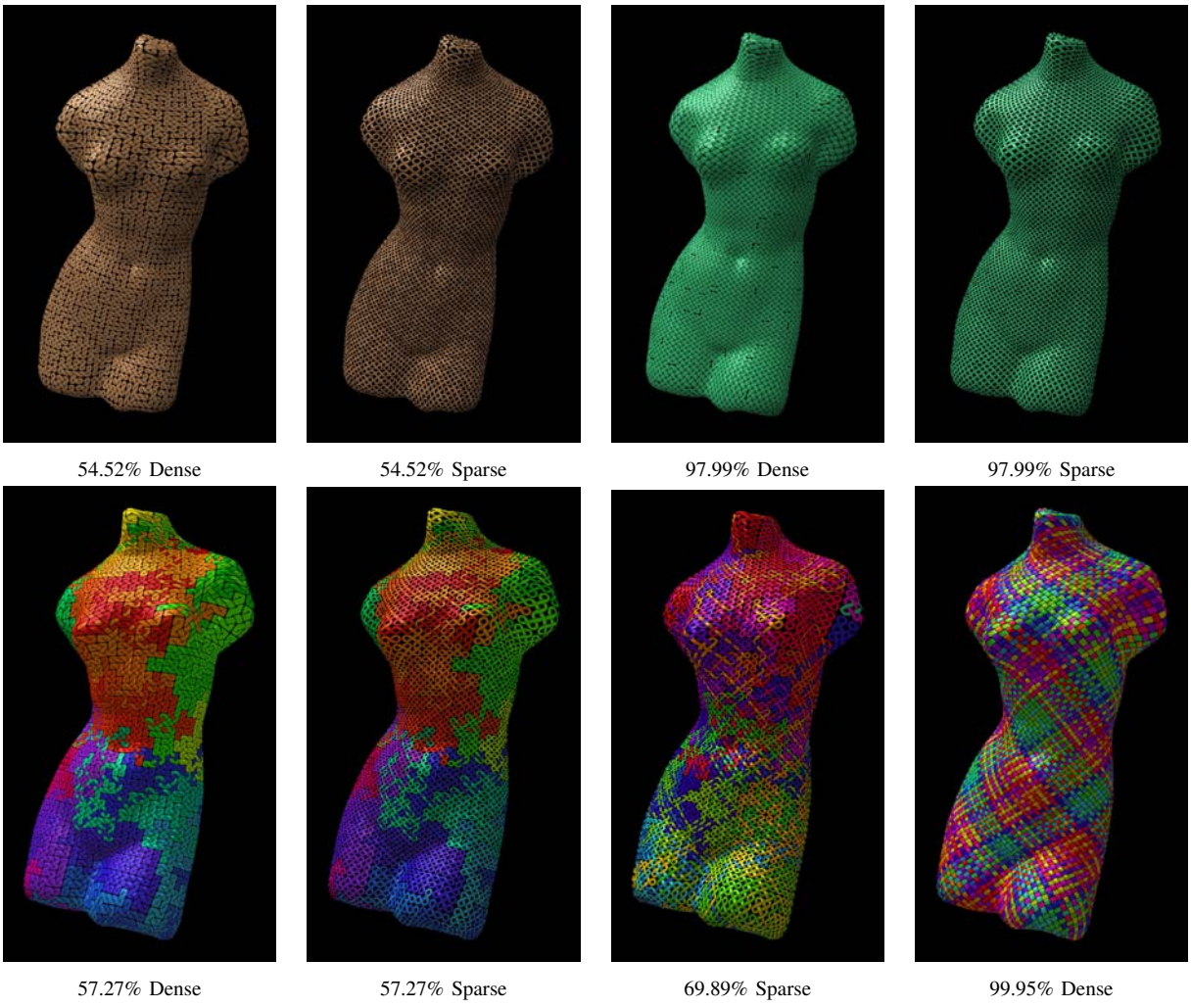

Fig. 8. *Single-cycle plain-woven Venus objects. Top images are uniform colored and bottom images are rainbow colored.*

intersection.

4. An Analysis of Single-Cycle Plain-Weaving

One might correctly expect that single-cycle graph rotation systems are sparsely distributed. An edge can be in either of two states: twisted or untwisted. If the number of edges is E, then, the total number of subsets of edges that could be selected for twisting is 2^E. Even if the proportion of single-cycle selections is very low, the absolute number of single-cycle selections can still be very high, as we shall see now.

4.1 Lower Bound from Spanning Trees of the Dual

A large set of single-cycle solutions on a mesh M with the smallest number of twisted edges can be obtained from the dual mesh $\overline{M}$ of the original mesh M. Note that each dual edge $\overline{e}$ between two vertices $\overline{v}_1$ and $\overline{v}_2$ in the dual mesh $\overline{M}$ corresponds to a primal edge e (i.e., an edge in the original mesh) M that is on the boundary of the two faces f_1 and f_2 in M. These two primal faces correspond to, respectively, the two dual vertices $\overline{v}_1$ and $\overline{v}_2$. Therefore, if we twist the primal edge e, then the two primal faces f_1 and f_2 are merged into a single face (Theorem 2.1). Correspondingly, the number of cycles in the corresponding weaving is reduced by one. Accordingly, if we construct a spanning tree $\overline{T}$ in the dual mesh $\overline{M}$, then twisting all the primal edges in M would merge all the faces in the original mesh M into a single face. This induces a single-cycle weaving. It is also easy to see that this is the minimum number of edges in M that must be twisted in order to obtain a single-cycle plain-weaving.

Let μ denote the average number of sides in a primal face (in the original mesh M) and let F denote the number of faces of M. Then it can be inferred from the dual of Euler's theorem (often called the edge-face equation) that the sum of the degrees of the vertices is twice the number of edges in a graph that $\mu F = 2E$. Therefore, the minimum number of edges that need to be twisted in order to obtain a single-cycle solution is

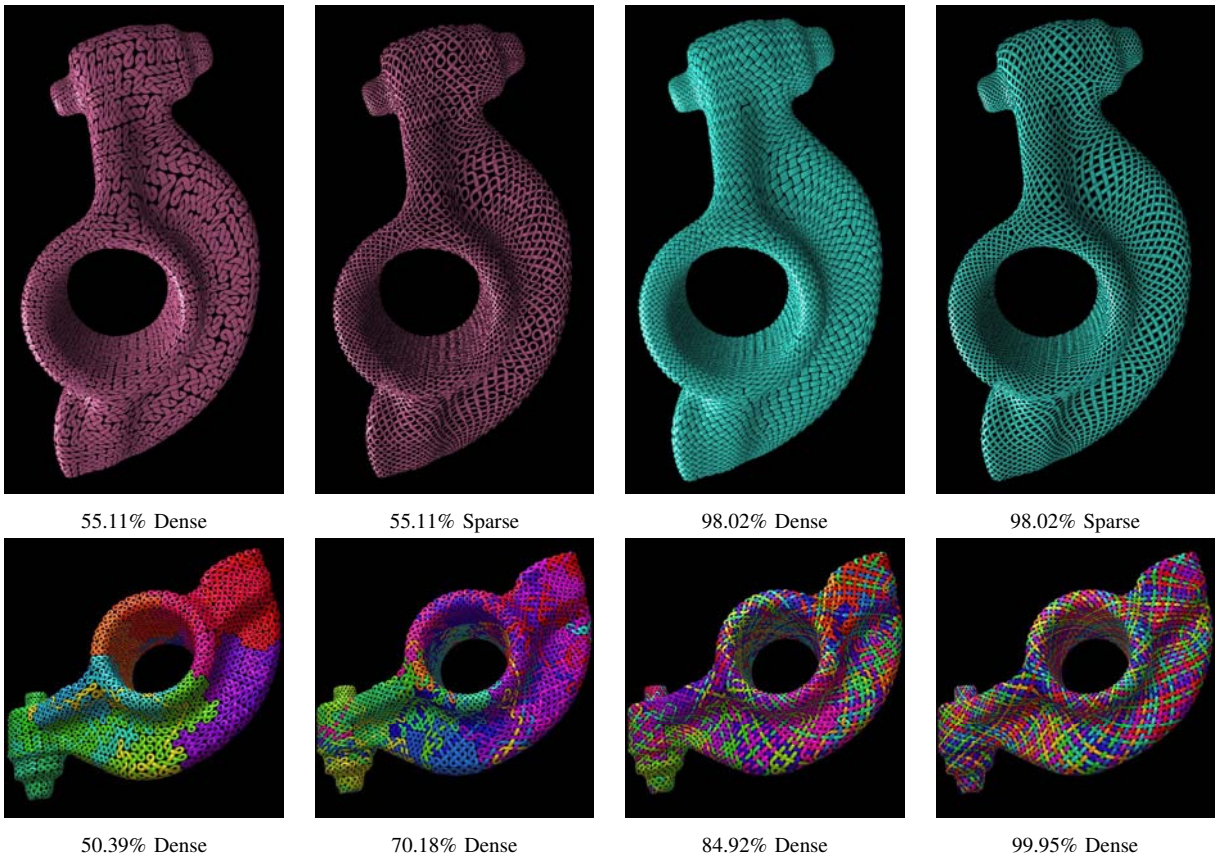

Fig. 9. *Single-cycle plain-woven Rockarm objects. Top images are uniform colored and bottom images are rainbow colored.*

the number of edges in a spanning tree of the dual graph, i.e.

$$F - 1 \;=\; \frac{2E}{\mu} - 1.$$

We also know (e.g. from Theorem 8.5.6 of [10]) that for large polyhedral meshes of any genus, the value of the average degree of a vertex and, dually, of the average number of sides of a face μ is at least 3 and at most a little more than 6. Therefore, we can safely predict that the minimum number of twisted edges lies between $0.33E$ and $0.66E$, depending on the type of the mesh. For $0.33E$, see Figure 11(b), which comes from a mostly hexagonal mesh, geodesic dome. Most of our examples in this paper are quadrilateral meshes, for which the minimum number of twists is $0.5E$. Of course, it is easy enough to construct a spanning tree in the dual graph, so we need not proceed by random selection of edges, if our sole objective is to obtain a single-cycle weaving.

4.2 Very Simple Statistical Analysis

We have randomly twisted edges for a large number of different types of meshes to understand the statistical behavior of the number of cycles (See Figures 2 and 13). Here, we will not provide a complete analysis. However, these trials confirm our theoretical assessment given earlier. As expected, the average number of cycles quickly drops when larger percentages of edges are twisted. As expected, random selection produces relatively few single-cycle embeddings. On the other hand, we obtained many 2-cycle and 3-cycle embeddings. Even this result is not unexpected. If no edge is twisted, then every face boundary walk on a polyhedral mesh is a cycle. Therefore, the maximum number of cycles is equal to the number of faces. Edge-twists combine face-cycles and thereby reduce the number of cycles dramatically. However, once the number of cycles becomes very low, some twists can separate a cycle into two, and thereby increase the number of cycles again. Therefore, although a low number of cycles is highly probable, a single-cycle embedding is not. On the other hand, there tend to be many single-cycle embeddings.

Given any embedding of a graph G, and given any spanning tree in the dual embedding, a single-cycle embedding can be obtained by twisting each edge of G whose dual lies in that spanning tree. Thus, the number of single-cycle embeddings is at least as large as the number of spanning trees in the dual.

If the dual graph is complete, then the number of spanning trees would be

$$\tau(G) = F^{F-2}$$

based on Cayley's formula, which is proved on page 155

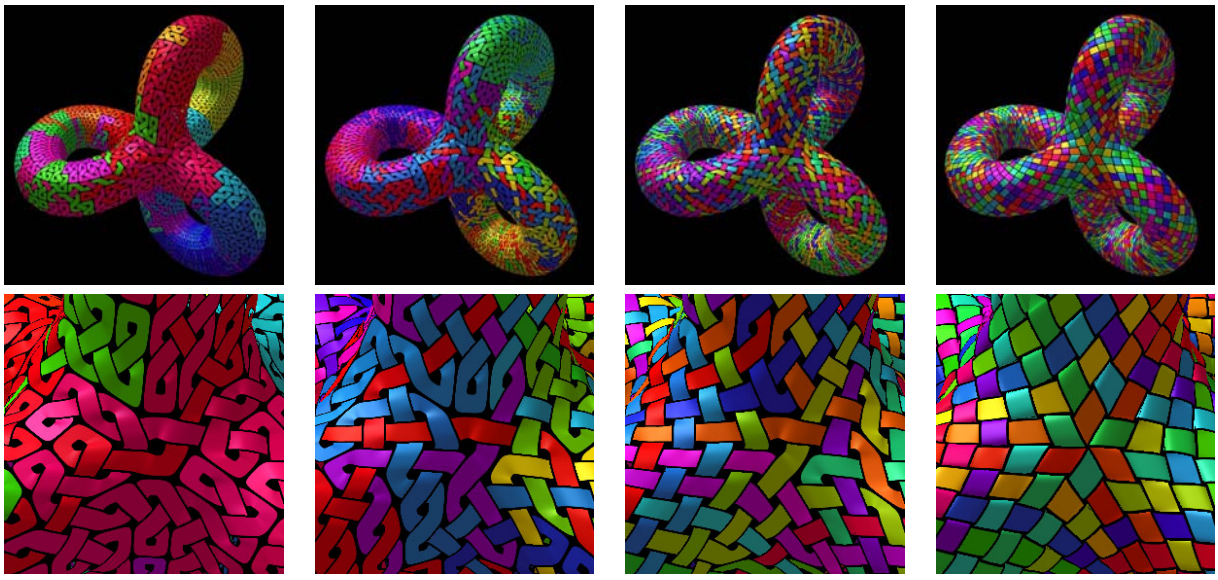

50.39% 69.60% 90.18% 99.96%

Fig. 10. *Rainbow colored single-cycle plain-woven genus-3 objects and details.*

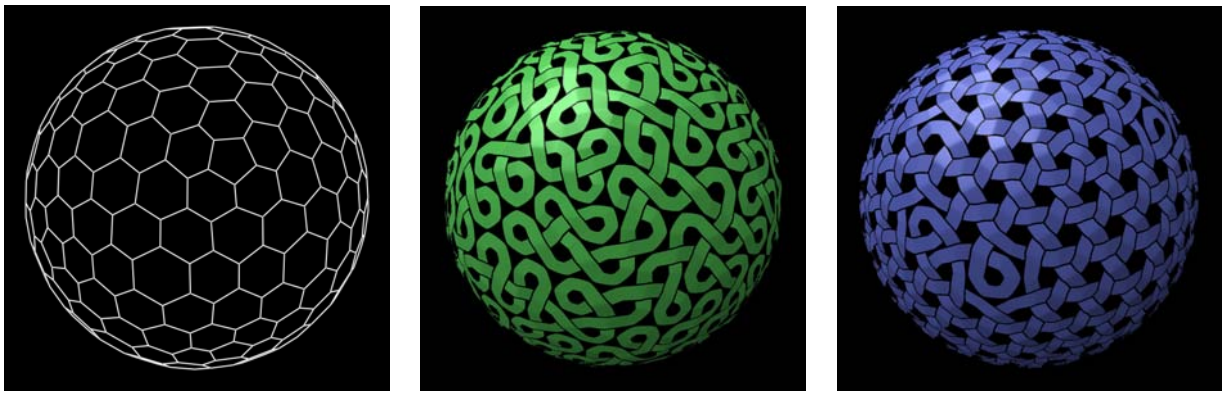

(a) Original Mesh (b) 33.52% (c) 96.41%

Fig. 11. *Uniform colored single-cycle plain-woven obtained from geodesic done.*

of [10]. More generally, there is a recursion for $\tau(G)$, the number of spanning trees of a graph G, which suggests a reason why the number of spanning trees is usually large. Let e be any proper edge. Then

$$\tau(G) = \tau(G - e) + \tau(G/e)$$

where $G-e$ is deletion and G/e is edge contraction. Of course, $\tau(G-e)$ counts the spanning trees of G that do not contain edge e, and $\tau(G/e)$ counts the spanning trees that do include e. Since a random graph G is 4-edge connected with probability 1, it follows from Kundu's theorem [11] that it has two disjoint spanning trees, which implies that deleting all the edges in one of them does not disconnect the graph. This implies that when the recursion is iterated over all the edges of one of the trees, all 2^{F-1} terms at the final level are positive. Thus, with probability 1, there are 2^{F-1} single cycle embeddings of G.

In summary, it is easy to obtain single-cycle embeddings. When we twist more than $F-1$ edges of a mesh, we usually obtain a low number of cycles. Then, twisting a few edges that are chosen to lie on the boundaries of two different cycles also brings us to a single-cycle embedding.

5. Conclusion, Future Work and Acknowledgments

We have shown that it is possible to create a single-cycle plain-weaving over any manifold mesh for any surface by selecting an appropriate subset of edges to be twisted. We have extended the original projection method of [Akleman2009mod1b] to handle untwisted edges. We have developed a system that transforms any manifold mesh into single-cycle plain-woven objects. The users simply provide a "reasonable" ratio of the edges that will be twisted. The system first randomly

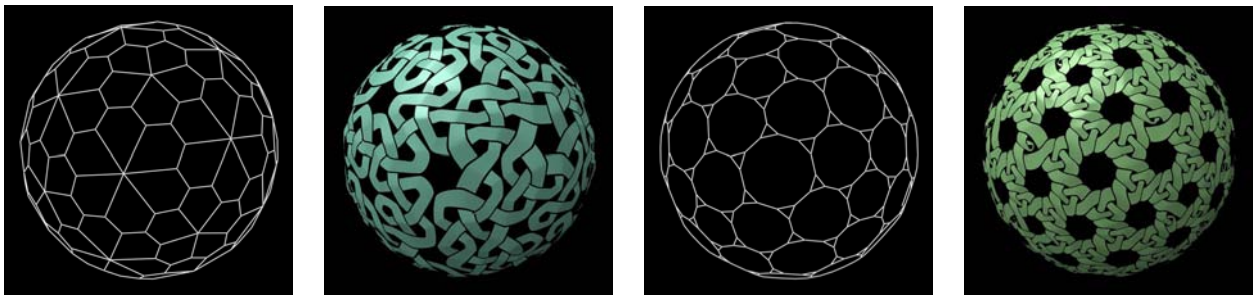

(a) Original Mesh (b) 52.22% (c) Original Mesh (d) 96.41%

Fig. 12. *Uniform colored single-cycle plain-woven obtained from 2 different tilings of a sphere.*

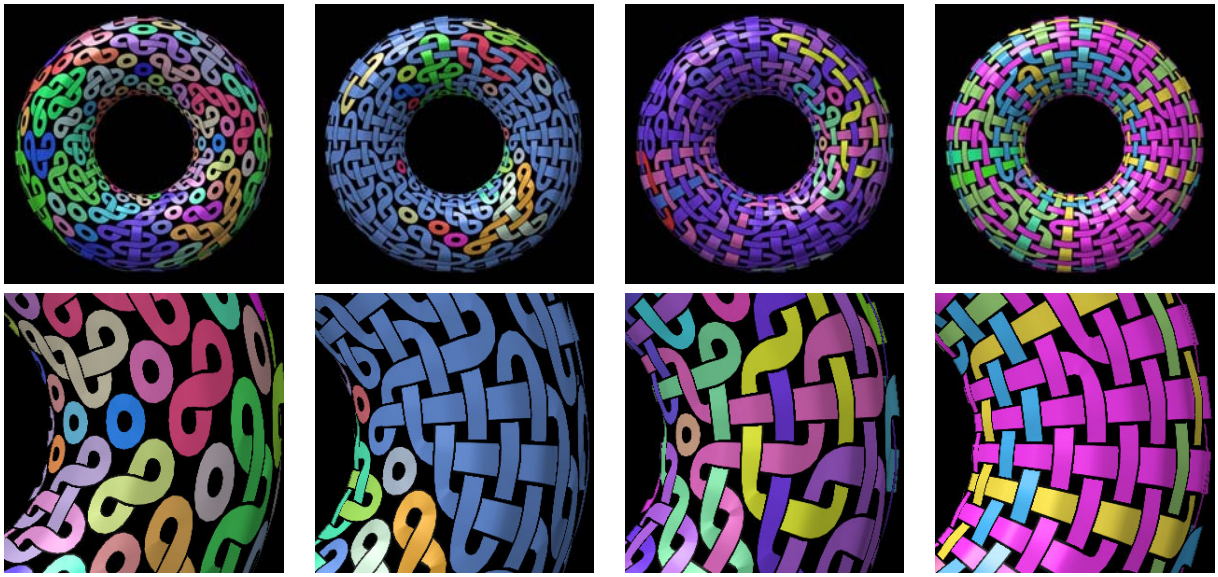

30% twisted
151 cycles

50% twisted
46 cycles

70% twisted
21 cycles

90% twisted
10 cycles

Fig. 13. *Random twisting with no cycle control. The numbers below indicate the percentage of edges that are twisted and the number of cycles. Each bottom images is magni cation of detail from the plain-woven Toroidal shapes immediately above. This illustrates how the percentage of twisted edges impacts the visual results.*

twists edges in the given ratio. Then, it twists and untwists[2] that are on the boundaries of two different cycles until it obtains a single-cycle embedding. This operation usually gives us a ratio which is reasonably close to the user-provided ratio.

We have shown that single-cycle embeddings for manifold meshes are not unique, and that there usually exist a large number of single-cycle plain-woven objects for any given orientable manifold mesh. Therefore, we expect that the same ideas can be used to create low number of cycles with interesting coloring patterns satisfying a given aesthetic requirement. Theoretically, the same results hold for non-orientable manifold meshes, but we have not yet implemented them in our system.

Single-cycle plain-woven objects are not necessarily as beautiful as multiple-cycle plain-woven objects, which can be more colorful, since for the former we can theoretically only use one color. Uniform-colored single-cycle woven objects, as shown in Figure 14 or top images in Figures 8 and 2, are not particularly exciting for their beauty, but, they are important in demonstrating that we can effectively control the number of cycles in a plain-weaving. With the suggestion of one of the reviewers we used a rainbow coloring scheme for painting the single-cycle ribbon with changing hue and the resulting images become both aesthetically pleasing and visually interesting by showing the structure of the cycle. We are particularly grateful to the anonymous reviewer who gave us this suggestion. We also thank the other anonymous reviewers for their helpful suggestions for the improvement of the paper.

[2]When it is possible, the system preferably alternates between twist and untwist by keeping the ratio unchanged.

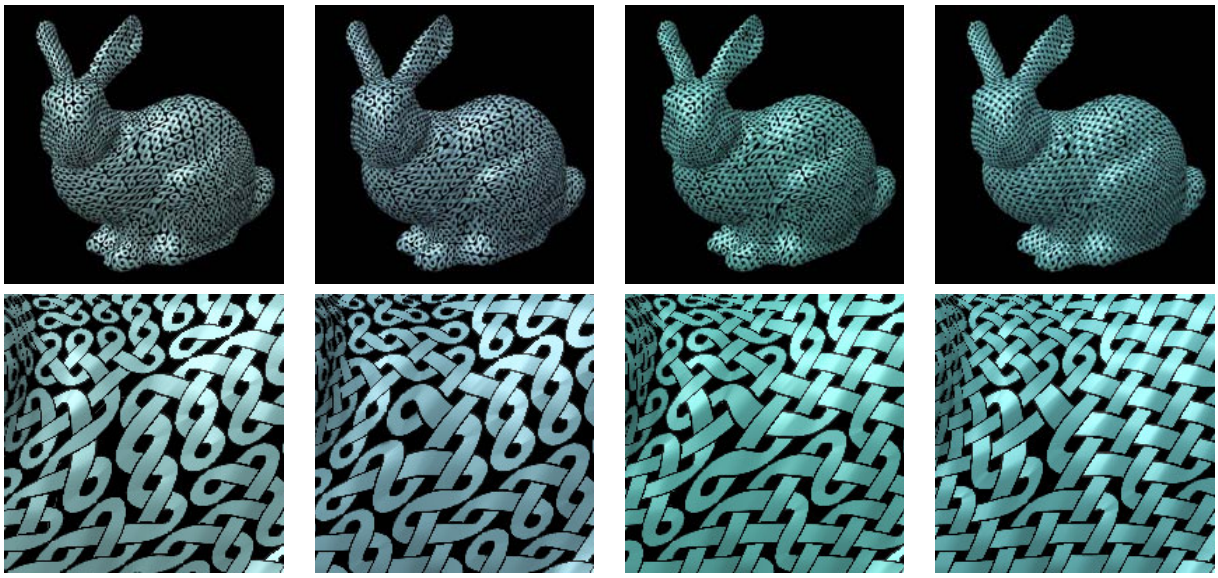

Fig. 14. *Uniform colored single-cycle plain-woven bunnies. Each bottom image magni es the detail of the single-cycle plain-woven bunny immediately above. The number below each bottom image indicates the percentage of edges that are twisted. These details illustrate how the percentage of twisted edges impacts the visual results.*

REFERENCES

[1] E. Akleman, J. Chen, Q. Xing, and J. Gross, "Cyclic plain-weaving on polygonal meshes with graph rotation systems," *ACM Transactions on Graphics; Proceedings of SIGGRAPH 2009*, pp. 78.1–78.8, 2009.

[2] E. Akleman, J. Chen, J. Gross, and Q. Xing, "Extended graph rotation systems as a model for cyclic weaving on orientable surfaces," Technical Report - Computer Science Department, Texas A&M University - TR09-203, 2009.

[3] C. Mercat, "Les entrelacs des enluminure celtes," *Dossier Pour La Science*, vol. 15, January 2001.

[4] M. Kaplan and E. Cohen, "Computer generated celtic design," in *Proc. of 14th Eurographics Workshop on Rendering*, 2003, pp. 9–16.

[5] J. L. Gross and T. W. Tucker, *Topological Graph Theory*. Wiley Interscience, New York, 1987.

[6] A. T. White, *Graphs of Groups on Surfaces, Volume 188: Interactions and Models*. North-Holland Mathematics Studies, 2001.

[7] C. P. Bonnington and C. H. C. Little, *The Foundations of Topological Graph Theory*. Springer, New York, 1995.

[8] J. Chen, J. L. Gross, and R. G. Rieper, "Overlap matrices and total imbedding distributions," *Discrete Mathematics*, no. 128, pp. 73–94, 1994.

[9] J. R. Edmonds, "On the surface duality of linear graphs," *Journal Res. Nat. Bur. Standards Sect. B*, pp. 121–123, 1965.

[10] J. L. Gross and J. Yellen, *Graph Theory and Its Applications*. 2nd Edition, CRC Press, 2006.

[11] S. Kundu, "Bounds on the number of disjoint spanning trees," *J. Combin. Theory Ser. B*, vol. 17, pp. 199–203, 1974.